REFERENCES

[1] J. M. Osepchuk, "Microwave engineering problems in the microwave oven," presented at 1976 IEEE MTT-S Int. Microwave Symp. Cherry Hill, NJ, June 14–16, 1976.

[2] H. Püschner, *Heating With Microwaves*. New York: Springer-Verlag, 1966, p. 176.

[3] S. Akhtarzad and P. B. Johns, "Analysis of a wide range of microwave resonators: T.L.M. methods," *Electron. Lett.* vol. 11, pp. 599–606, Nov. 27, 1975.

[4] N. Marcuvitz, *Waveguide Handbook*. New York: McGraw-Hill, 1951, p. 17.

[5] A. R. Von Hippel, *Dielectric Materials and Applications*. New York: Wiley, 1954, p. 361.

[6] N. Marcuvitz, *Waveguide Handbook*. New York: McGraw-Hill, 1951, pp. 388–393.

[7] W. S. Ataras, "The field solution for a partially filled cavity," unpublished.

[8] S. Ramo and J. R. Whinnery, *Fields and Waves in Modern Radio*. New York: Wiley, 1944, p. 395.

Characteristics of Single and Coupled Microstrips on Anisotropic Substrates

NICOLAOS G. ALEXOPOULOS, MEMBER, IEEE, AND CLIFFORD M. KROWNE, MEMBER, IEEE

Abstract—**In this paper, the effect of an anisotropic substrate on the characteristics of covered microstrip is presented for single and coupled lines. The Green's function is obtained in integral and series form for an arbitrary anisotropic substrate. Computer programs based on the method of moments approach [1], [2] are employed and results are presented in graphical form for impedance Z, coupling constant K, and phase velocity v_p as functions of n_x/n_y (the ratio of the substrate indices of refraction). Z, K, and v_p are studied for various w/H, S/H, and B/H ratios where w is the line width (w_1 and w_2 for coupled lines), S is the separation between coupled lines, B is the separation between ground planes, and H is the substrate thickness.**

I. INTRODUCTION

EXTENSIVE results exist in the literature on the problem of microstrip lines on isotropic substrates, e.g., [1]–[13]. Therein, the Green's function of the problem is obtained either by image theory [7] or by a direct solution to the boundary value problem [13]. In most cases a quasi-static approach is presented, which necessitates solution to Laplace's equation for a given set of boundary conditions. A series of papers [8]–[12] presents solutions to the dispersion problem, again for isotropic substrates.

Recently [14], [15], the problem of anisotropic substrates was approached strictly from the numerical point of view. Specifically, the authors employed the method of finite differences to obtain the impedance characteristics of a single microstrip line over a single-crystal sapphire substrate. Since this crystal is uniaxial, the permittivity dyadic is strictly diagonal with a relative permittivity along the optical axis $\epsilon_y = 11.60$, while on the plane perpendicular to this axis $\epsilon_x = \epsilon_z = 9.40$. The authors proceeded to compute an equivalent isotropic relative permittivity ϵ_{req} which enables them to proceed with the computations of the microstrip characteristics.

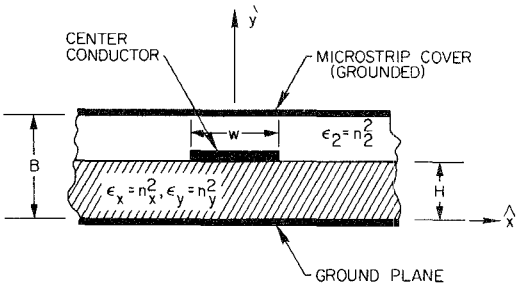

Fig. 1. Cross section of covered single microstrip geometry.

In the present paper, the problem of the anisotropic substrate is approached from the boundary value point of view. The boundary value approach necessitates the introduction of a grounded cover, although this by no means limits the usefulness of the solution since B (see Fig. 1) can be allowed to recede to infinity. An image theory approach would be much more preferable, but there appears to be no prior references on how conductors image over anisotropic media. By employing a quasi-static approach, the Green's function is incorporated into two methods of moments computer programs. These programs provide solutions to the single and coupled microstrip problem by employing the usual methods for the computation of self and mutual capacitances, characteristic impedances, and phase velocities. The results are presented for various values of the relative permittivities in the x, y, and z directions, and they are shown in Figs. 2–4 and 6 and 7.

Manuscript received August 30, 1976; revised July 15, 1977. This work was supported jointly by the U.S. Office of Naval Research under Contract N00014-76C-0896 and by the Watkins–Johnson Company.

N. G. Alexopoulos is with the Department of Electrical Sciences and Engineering, University of California, Los Angeles, CA 90024.

C. M. Krowne is with the Watkins–Johnson Company, Palo Alto, CA 94304.

0018-9480/78/0600-0387$00.75

II. Green's Function for an Anisotropic Substrate

The geometry of Fig. 1 is considered where a charged line of ρ_l C/m is assumed parallel to the $\hat{z}$ axis at $y=H$. The space $H<y<B$ is assumed homogeneous and isotropic with a relative permittivity ϵ_2. For $0<y<H$ (the substrate region), the medium is anisotropic and oriented in such a manner that the relative permittivity is given by the following dyadic:

$$\bar{\bar{\epsilon}}=\begin{bmatrix} \epsilon_x\hat{x}\hat{x} & 0 & 0 \\ 0 & \epsilon_y\hat{y}\hat{y} & 0 \\ 0 & 0 & \epsilon_z\hat{z}\hat{z} \end{bmatrix}. \tag{1}$$

A quasi-static solution to the potential problem can be obtained by solving Laplace's equations in the two dielectric regions subject to the proper boundary conditions. One needs to solve in the anisotropic region the equation

$$\nabla\cdot\left(\bar{\bar{\epsilon}}\cdot\nabla\phi_1\right)=0. \tag{2}$$

Due to the infinite extent of the line in the z direction, the problem is two dimensional. Therefore, (2) yields

$$\epsilon_x\frac{\partial^2\phi_1}{\partial x^2}+\epsilon_y\frac{\partial^2\phi_1}{\partial y^2}=0 \tag{3}$$

which has a solution of the form

$$\phi_1(x,y)=\left[a_1(k)\cos\left(\frac{kx}{n_x}\right)+b_1(k)\sin\left(\frac{kx}{n_x}\right)\right]\cdot\left[c_1(k)\sinh\left(\frac{ky}{n_y}\right)+d_1(k)\cosh\left(\frac{ky}{n_y}\right)\right] \tag{4}$$

with k being a continuous variable. Because of the even symmetry in x and the fact that at the ground plane $\phi_1(x,0)=0$, it follows that the general solution of (3) can be written as

$$\phi_1(k)=\int_{-\infty}^{\infty}A_1(k)\cos\left(\frac{kx}{n_x}\right)\left\{\frac{\sinh\left(ky/n_y\right)}{\sinh\left(kH/n_y\right)}\right\}dk \tag{5}$$

where $n_x=(\epsilon_x)^{1/2}$ and $n_y=(\epsilon_y)^{1/2}$. Using Laplace's equation in the isotropic region ($H<y<B$), i.e.,

$$\nabla^2\phi_2=0 \tag{6}$$

one must obtain $\phi_2(x,y)$ such that $\phi_2(x,B)=0$ at the top ground plane and

$$\phi_1(x,y)|_{y=H^-}=\phi_2(x,y)|_{y=H} \tag{7}$$

while satisfying the boundary condition

$$\hat{y}\cdot\left(\bar{D}_1-\bar{D}_2\right)=-\rho_l\delta(x). \tag{8}$$

Normalizing the x and y variables in (6) to the same constant n_x, a general solution in region 2 is obtained in the form

$$\phi_2(x,y)=\int_{-\infty}^{\infty}A_2(k)\cos\left(\frac{kx}{n_x}\right)\left\{\frac{\sinh\left(k(B-y)/n_x\right)}{\sinh\left(k(B-H)/n_x\right)}\right\}dk. \tag{9}$$

From the continuity of potentials at $y=H$, it follows that $A_1(k)=A_2(k)=A(k)$. By employing the boundary condition at $y=H$ which is expressed in (8), it follows that

$$\rho_l\delta(x)=\int_{-\infty}^{\infty}A(k)\cos\left(\frac{kx}{n_x}\right)\cdot\left\{n_y\coth\left(\frac{kH}{n_y}\right)+\frac{n_2^2}{n_x}\coth\left[\frac{k(B-H)}{n_x}\right]\right\}k\,dk. \tag{10}$$

Since

$$\int_{-\infty}^{\infty}\cos\left(\frac{kx}{n_x}\right)dk=2\pi\delta\left(\frac{x}{n_x}\right)=2\pi n_x\delta(x) \tag{11}$$

$A(k)$ is obtained from (10) in the form

$$A(k)=\frac{\rho_l}{2\pi\epsilon_0}\cdot\left\{\frac{1}{k}\left(\frac{1}{n_xn_y\coth\left(kH/n_y\right)+n_2^2\coth\left[k(B-H)/n_x\right]}\right)\right\}. \tag{12}$$

Here ϵ_0 is the permittivity of a vacuum. The potential is now given by

$$\phi_1(x,y)=\frac{\rho_l}{2\pi\epsilon_0}\int_{-\infty}^{\infty}\frac{dk}{k}\;\frac{\cos\left(kx/n_x\right)\sinh\left(ky/n_y\right)}{\left\{n_xn_y\cosh\left(kH/n_y\right)+n_2^2\sinh\left(kH/n_y\right)\coth\left[k(B-H)/n_x\right]\right\}} \tag{13}$$

for $0\leqslant y\leqslant H$, and by

$$\phi_2(x,y)=\frac{\rho_l}{2\pi\epsilon_0}\int_{-\infty}^{\infty}\frac{dk}{k}\;\frac{\cos\left(kx/n_x\right)\sinh\left[k(B-y)/n_x\right]}{\left\{n_xn_y\sinh\left(k(B-H)/n_x\right)\coth\left(kH/n_y\right)+n_2^2\cosh\left(k(B-H)/n_x\right)\right\}} \tag{14}$$

for $H\leqslant y\leqslant B$.

If $\rho_l = 1$ and $y = H$, the Green's function for the microstrip over an anisotropic substrate is expressed simply by the equation

$$\phi(x,H) = \frac{1}{2\pi\epsilon_0}\int_{-\infty}^{\infty}\frac{dk}{k} \cdot \frac{\cos(kx/n_x)}{\{n_x n_y \coth(kH/n_y) + n_2^2 \coth(k(B-H)/n_x)\}}. \quad (15)$$

III. Numerical Analysis

In order to compute the characteristic impedance Z, phase velocity v_p, and coupling constant K parameters of the microstrip, a numerical approach based on the method of moments has been employed. Two computer programs have been developed to compute $\phi(x,H)$ in (15). The first one simply evaluates (15) using a numerical integration approach [16]. This entails separating the integration interval into two ranges: Δ to P and P to ∞. If P is chosen large enough, the coth functions will approach one and the integration can be represented as follows:

$$\phi(x,H) = \frac{1}{\pi\epsilon_0}\int_{\Delta}^{P}\frac{dk}{k} \cdot \frac{\cos(kx/n_x)}{\{n_x n_y \coth(kH/n_y) + n_2^2 \coth(k(B-H)/n_x)\}} + \frac{1}{\pi\epsilon_0(n_x n_y + n_2^2)}\int_{P}^{\infty}\frac{dk}{k}\cos\left(\frac{kx}{n_x}\right). \quad (16)$$

In order for (16) to approximate $\phi(x,H)$ well, $\Delta \to 0$ and P must be such that the coth arguments $\theta_a \geq 6$. The lower limit in the first integral is not set $\Delta \equiv 0$ because the coth functions blow up at $k = 0$, preventing a correct numerical evaluation. The second integral in (16) can be calculated using the IBM scientific subroutine package program SICI.

The first integral can be determined using a Simpson integration routine. The cos argument increment $|\Delta\theta_c$ must be chosen small enough to approximate the cos oscillation behavior, $\Delta\theta_c \leq 5°$. This $\Delta\theta_c$ value specifies the k integration interval $\Delta k = n_x \Delta\theta_c / x$.

The other computer program computes $\phi(x,H)$ in (15) through a series expression (19) derived as follows. By analytic continuation, $\phi(x,H)$ in (15) can be rewritten as

$$\phi(x,H) = \frac{1}{2\pi\epsilon_0}\,\mathrm{Re}\oint_C \frac{dz}{z} \cdot \frac{\exp(i(x/n_x)z)}{\left[n_x n_y \coth(Hz/n_y) + n_2^2 \coth\left[((B-H)/n_x)z\right]\right]} \quad (17)$$

where z is a complex variable and C is the path of integration which extends from $-\infty$ to $+\infty$ along the Re (z) axis and closes on the upper half z plane. It can be easily demonstrated that $z = 0$ is an ordinary point, and that there exists an infinite number of poles restricted to the Im (z) axis. By invoking the residue theorem, $\phi(x,H)$ can be rewritten as

$$\phi(x,H) = \frac{1}{\epsilon_0}\,\mathrm{Re}\sum_{p=1}^{\infty} iQ_p \quad (18)$$

where Q_p denotes the residue at the pth pole. In accordance with this approach, the residue series yields

$$\phi(x,H) = \frac{1}{\epsilon_0}\sum_{p=1}^{\infty} \cdot \frac{\exp(-(|x|r_p/n_x))}{r_p H\left[n_x \csc^2(Hr_p/n_y) + n_2^2(\nu/n_x)\csc^2((H\nu/n_x)r_p)\right]} \quad (19)$$

where $\nu = (B/H) - 1$ and r_p is the pth zero of the determinantal equation

$$\frac{\cot(Hr/n_y)}{\cot(H\nu r/n_x)} = -\frac{n_2^2}{n_x n_y}. \quad (20)$$

Of interest is the special case where $n_x = n_y = n_1$, i.e., that of isotropic substrate. In this case, the parameter ν is of importance in locating the roots of r_p properly. For example, if $\nu = 1$, (19) simplifies to

$$\phi(x,H) = \frac{2}{\epsilon_0}\sum_{p=1}^{\infty}\frac{\exp(-(|x|/2\pi)p\pi)}{p\pi\left[n_1^2 + n_2^2\right]} \quad (21)$$

which agrees with the result obtained for isotropic substrates by Farrar and Adams [2].

In order to verify the accuracy of our computer programs, extensive computations were performed based on the Green's function given by (16) and (19). Using (19), agreement within 5 percent was found with the results of [2] for all cases of B/H and w/H for $\epsilon_x = \epsilon_y = 9.6$, as well as with the results of [3] for alumina with $\epsilon_x = \epsilon_y = 9.9$ and $B/H = 6$. For example, the case $B/H = 6$, $w/H = 1.0$, and $\epsilon_x = \epsilon_y = 9.6$ yields $Z = 48.73\ \Omega$ ($N = 20$ partitions/line using ANIGREEN 1) and 48.4 Ω from [2]. This is a discrepancy of 0.7 percent. (Note that $n_2 = 1$. This is true throughout our paper.) In addition, the special case of a single-crystal sapphire substrate with $\epsilon_x = 9.40$ and $\epsilon_y = 11.60$ was examined. In this latter case, our results agree within about 5 percent of the values obtained in [14] for Z versus w/H. Figs. 2(a) and (b) show a comparison of the characteristic impedance Z and normalized phase velocity v_p/c versus w/H for alumina substrates with $B/H = 6$ (c = velocity of light in a vacuum). Fig. 2(a) indicates that the values of the characteristic impedance Z are quite close for polycrystalline and single-crystal aluminas; in fact, for $w/H > 4.5$, the two curves coalesce. On the other hand, the two alumina materials exhibit divergent phase velocity characteristics as evidenced by Fig. 2(b). This latter observation underlines the fact that more precise documentation of anisotropic substrate properties is required. To this end, computations for microstrip over anisotropic substrates have been performed for both single (Section IV) and coupled (Section V) microstrip lines. The calculations in the next two sections are performed using (19) for loosely coupled or uncoupled lines (computer program ANIGREEN 1, see [17]) and (16) for tightly coupled lines (computer program ANIGREEN 2,

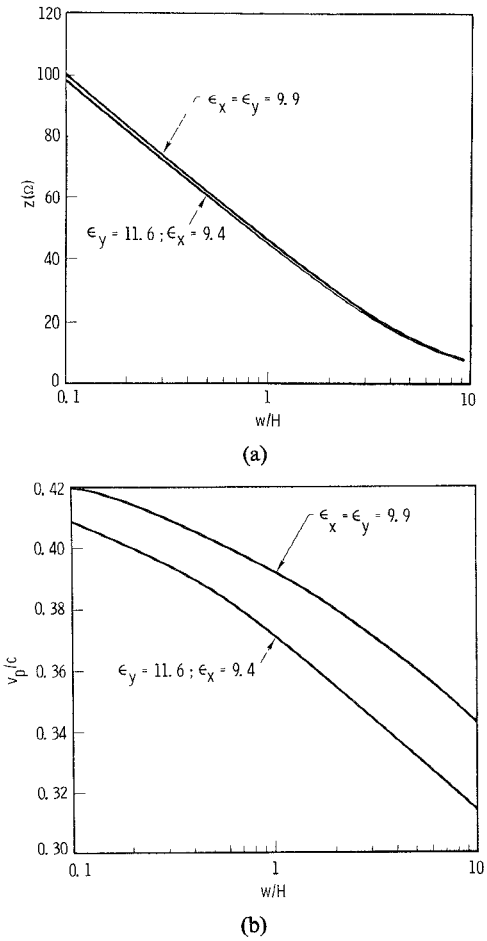

Fig. 2. (a) Single microstrip characteristic impedance Z versus $w/H(B/H=6)$ for alumina substrates. (b) Single microstrip phase velocity v_p/c (normalized to c) versus $w/H(B/H=6)$ for alumina substrates.

see [17]). Equation (16) yields coupled line parameters which have been found to agree within 5 percent of the alumina results found in [6]. Equation (16) also yields results within 5 percent of Bryant and Weiss' computer program MSTRIP [18]. (The computer program accuracy is increased by increasing the number of partitions into which the line is subdivided.)

IV. Single Microstrip Characteristics

Figs. 3(a), (b), and (c) show the behavior of Z versus n_x/n_y for $w/H=0.1$, 1, and 10, respectively, with $B/H=6$. In Fig. 3(a), the relative permittivity values are normalized to $\epsilon_y=9.9$, which is the relative permittivity usually employed in the literature for alumina substrates. It is observed that, as w/H increases in value from 0.1 to 10.0, the value of Z drops considerably for all n_x/n_y. This behavior parallels that found in isotropic substrates where, as w increases, a greater portion of the electric field lines are in the substrate as opposed to the air, increasing the effective dielectric constant and thereby decreasing Z. For a given w/H, Z decreases as n_x/n_y increases. This is due to an increase in the electric field lines in the x direction E_x with rising n_x or ϵ_x since n_y is fixed. The slope of the curves goes down with rising w/H since $E_y \gg E_x$.

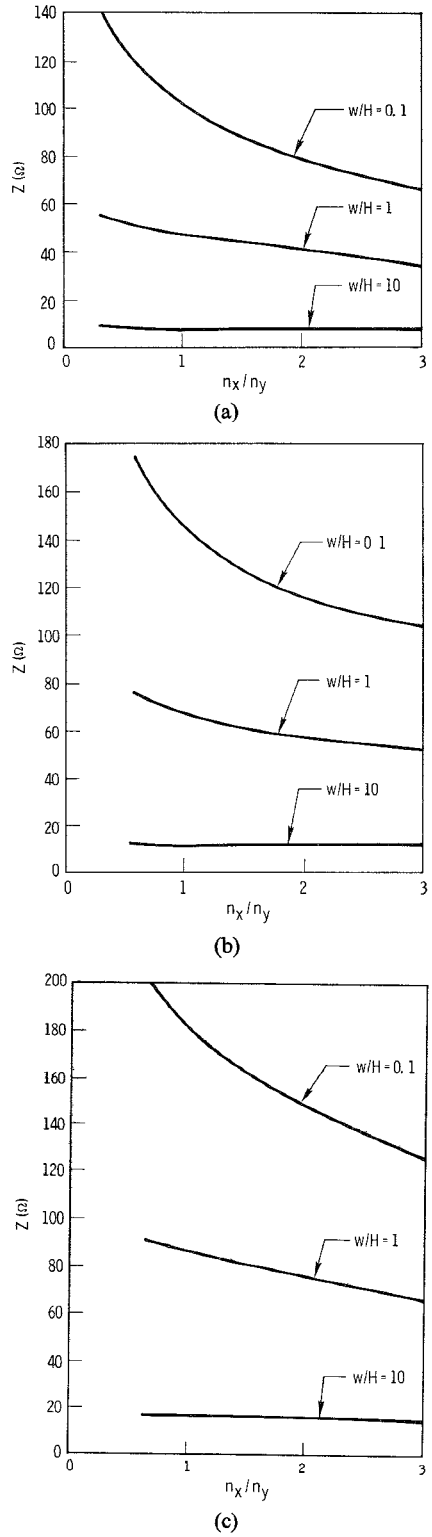

Fig. 3. (a) Z versus n_x/n_y for alumina-like substrates; $B/H=6$ (permittivity tensor normalized to $\epsilon_y=9.9$). (b) Z versus n_x/n_y for quartz-like substrates; $B/H=6$ (permittivity tensor normalized to $\epsilon_y=4.5$). (c) Z versus n_x/n_y for polystyrene-like substrates; $B/H=6$ (permittivity tensor normalized to $\epsilon_y=2.55$).

Figs. 3(b) and (c) show the characteristic impedance behavior for quartz-like (SiO material) and polystyrene-like substrates with the permittivity tensor elements being normalized to, respectively, $\epsilon_y=4.5$ and $\epsilon_y=2.55$. One notices that for a particular w/H value, Z increases in

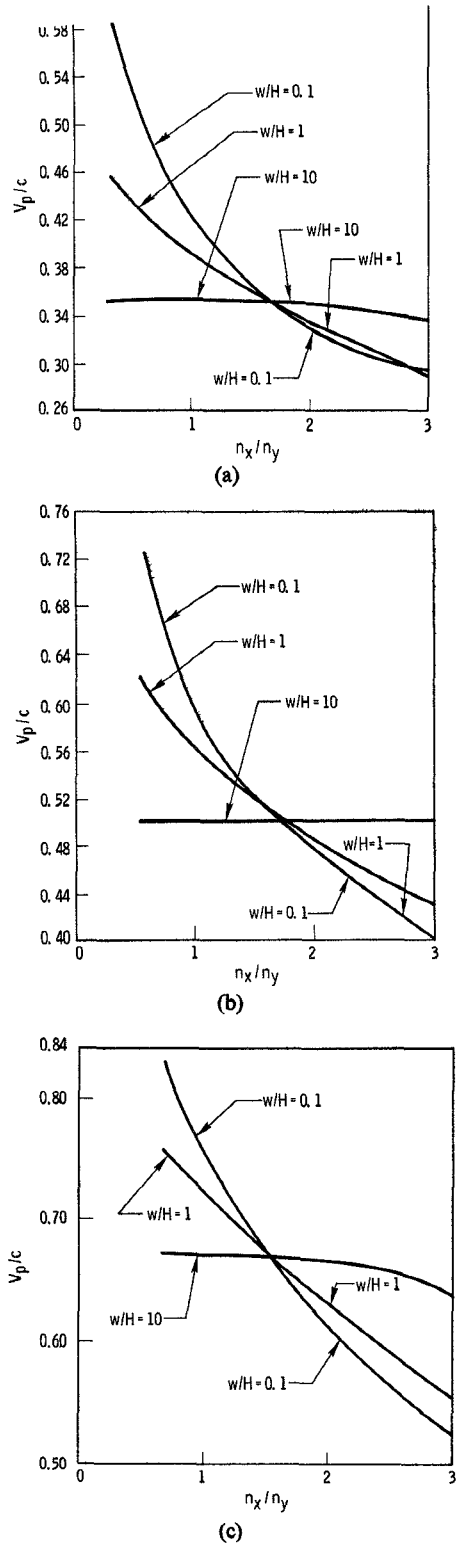

Fig. 4. (a) v_p/c versus n_x/n_y for alumina-like substrates; $B/H=6$ (permittivity tensor normalized to $\epsilon_y=9.9$). (b) v_p/c versus n_x/n_y for quartz-like substrates; $B/H=6$ (permittivity tensor normalized to $\epsilon_y=4.5$). (c) v_p/c versus n_x/n_y for polystyrene-like substrates; $B/H=6$ (permittivity tensor normalized to $\epsilon_y=2.55$).

going from Fig. 3(a) to 3(c) (with n_y getting smaller), because n_y controls E_y and therefore Z.

In Figs. 4(a), (b), and (c), the normalized phase velocity v_p/c is shown for $w/H=0.1$, 1, and 10 with $B/H=6.0$.

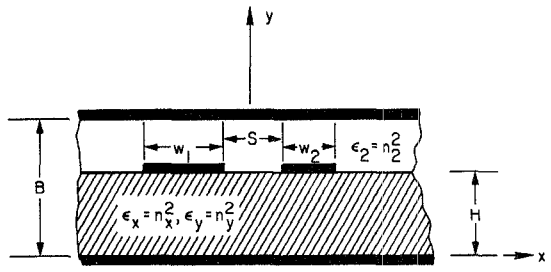

Fig. 5. Cross section of covered coupled microstrip lines geometry.

As expected, these curves show lower v_p/c values for all w/H as the normalizing parameter ϵ_y increases. Also, as w/H increases, it is clear that v_p/c changes very slowly as n_x/n_y increases and in fact, for quartz-like substrates, $v_p/c \cong 0.50$ when $n_x/n_y \geq 1$ $(w/H=10)$.

V. Coupled Microstrip Characteristics

The characteristic impedance, phase velocity, and coupling constant parameters of coupled pairs of microstrip transmission lines are presented here for anisotropic substrates. The microstrip conductors are assumed to be parallel to the $\hat{z}$ direction, separated by a distance S and, in general, of unequal widths w_1, w_2, as shown in Fig. 5. The even- and odd-mode properties of the coupled microstrip have been obtained by employing the same approach which is customary in numerous quasi-static TEM studies of isotropic substrates, and therefore the analysis will not be reproduced here [6]. Our results are confined to alumina-like substrates [17]. Figs. 6(a) and (b) show the even- and odd-mode impedance and phase velocity plotted versus n_x/n_y. The results are for $B/H=20$, $w/H=1$, and $S/H=0.25$ with the permittivity tensor being normalized to $\epsilon_y=9.9$. As in the case of isotropic substrates, there exist large differences in characteristic impedance values between the even and odd modes for small S/H. This is evidenced in Fig. 6(a) where the even-mode impedance Z_e is larger than the odd-mode impedance Z_o by roughly 25 Ω for all values of n_x/n_y. On the other hand, contrary to the isotropic substrate results, the normalized phase velocity curves v_p/c for the even (v_{pe}) and odd (v_{po}) modes converge to $v_{po}/c \cong 0.334$ and $v_{pe}/c \cong 0.320$ values for $n_x/n_y \cong 2.0$. This indicates that $v_{po}-v_{pe}$ can be minimized for the proper value of n_x/n_y. Fig. 6(c) shows that the coupling K rises with n_x/n_y as expected, due to increasing E_x. K was calculated by employing the formula [19]

$$K=\frac{G}{\sqrt{AB}} \tag{22}$$

with

$$G=\frac{Z_{o1}^{-1}-Z_{e1}^{-1}}{2}=\frac{Z_{o2}^{-1}-Z_{e2}^{-1}}{2} \tag{23}$$

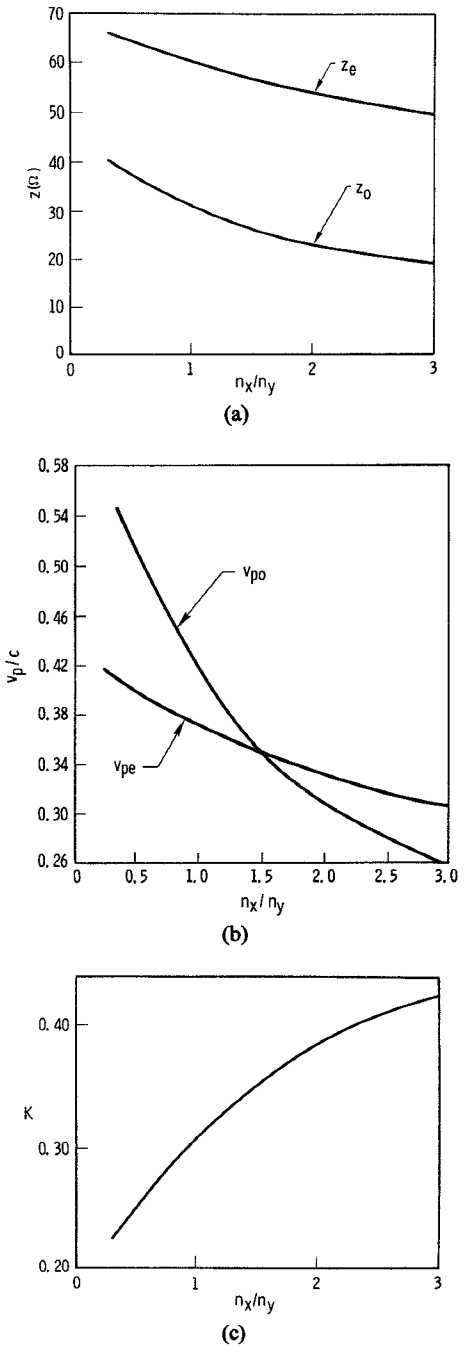

Fig. 6. (a) Even- and odd-mode impedances Z_e and Z_o versus n_x/n_y for parallel-coupled microstrip on an anisotropic alumina-like substrate ($\bar{\epsilon}$ normalized to $\epsilon_y = 9.9$). $w/H = 1$, $S/H = 0.25$, and $B/H = 20$. (b) v_{pe} and v_{po} versus n_x/n_y for parallel-coupled microstrip on an anisotropic alumina-like substrate ($\bar{\epsilon}$ normalized to $\epsilon_y = 9.9$). $w/H = 1$, $S/H = 0.25$, and $B/H = 20$. (c) Coupling constant K versus n_x/n_y for parallel microstrip on an anisotropic alumina-like substrate ($\bar{\epsilon}$ normalized to $\epsilon_y = 9.9$). $w/H = 1$, $S/H = 0.25$, and $B/H = 20$.

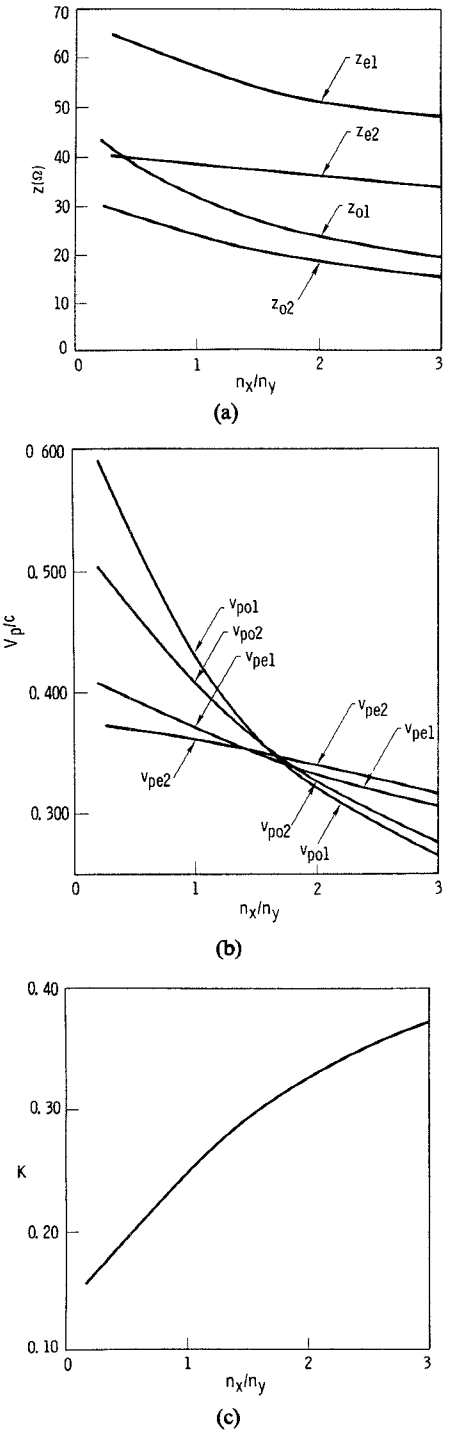

Fig. 7. (a) Even- and odd-mode impedances Z_{e1}, Z_{e2}, Z_{o1}, and Z_{o2} versus n_x/n_y for parallel-coupled microstrip on an anisotropic alumina-like substrate ($\bar{\epsilon}$ normalized to $\epsilon_y = 9.9$). $w_2/H = 1$, $w_2/H = 2$, $S/H = 0.25$, and $B/H = 20$. (b) Even- and odd-mode phase velocities v_{e1}, v_{e2}, v_{o1}, and v_{o2} versus n_x/n_y for parallel-coupled microstrip on an anisotropic alumina-like substrate ($\bar{\epsilon}$ normalized to 9.9). $w_1/H = 1$, $w_2/H = 2$, $S/H = 0.25$, and $B/H = 20$. (c) K versus n_x/n_y for parallel-coupled microstrip on an anisotropic alumina-like substrate ($\bar{\epsilon}$ normalized to $\epsilon_y = 9.9$). w_1 substrate ($\bar{\epsilon}$ normalized to $\epsilon_y = 9.9$). $w_1/H = 1$, $w_2/H = 2$, $S/H = 0.25$, and $B/H = 20$.

and

$$A = \frac{Z_{o1}^{-1} + Z_{e1}^{-1}}{2}$$

$$B = \frac{Z_{o2}^{-1} + Z_{e2}^{-1}}{2}. \tag{24}$$

Figs. 7(a), (b), and (c) demonstrate the characteristics of coupled microstrip lines which are of unequal width; here, $w_1/H = 1$ and $w_2/H = 2$. $S/H = 0.25$, $B/H = 20$, and $\epsilon_y = 9.9$, as we had in Figs. 6(a), (b), and (c). The unequal line widths cause the even- and odd-mode curves of Figs. 6(a), (b), and (c) to split up into Z_{o1}, Z_{o2}; Z_{e1}, Z_{e2}; v_{po1}, v_{po2}; and v_{pe1}, v_{pe2}. In Fig. 7(b), all phase velocities approach one another near $n_x/n_y = 1.6$. They are within one percent of

each other at this point. In general, for unequal but arbitrary line widths one does not expect the solution to yield a point where all v_p are equal or nearly equal.

VI. Discussion

Here we have demonstrated the effect of substrate anisotropy on the single and coupled microstrip line characteristics Z, v_p, and K, assuming a quasi-static TEM solution to hold. It is found for coupled lines that by properly choosing the substrate material, the difference between even- and odd-mode phase velocities can be significantly reduced compared to using isotropic or nearly isotropic substrates. This implies that the isolation and directivity of microstrip couplers can be markedly improved. One should also be able to improve the performance of microstrip filters.

An example of a substance which possesses enough anisotropy to make it a feasible substrate material to demonstrate an improvement in directivity of couplers due to a minimization in $v_{po} - v_{pe}$ is pyrolytic boron nitride (PBN). This crystal is currently being studied theoretically and experimentally at Watkins–Johnson Company [20].

Acknowledgment

C. M. Krowne would like to thank Dr. E. J. Crescenzi, Jr., for suggesting that he study the effect of anisotropy on microstrip waveguide electrical parameters, and R. C. Helvey for helping the author with a number of computational problems, both of Watkins–Johnson Company. The authors would also like to thank S. Kerner of the University of California, Los Angeles, for assisting with some of the numerical calculations.

References

[1] A. Farrar and A. T. Adams, "Characteristic impedance of microstrip by the method of moments," *IEEE Trans. Microwave Theory Tech.*, vol. MTT-18, pp. 65–66, Jan. 1970.

[2] ——, "A potential theory method for covered microstrip," *IEEE Trans. Microwave Theory Tech.* vol. MTT-21, pp. 494–496, July 1973.

[3] E. Yamashita, "Variational method for the analysis of microstrip-like transmission lines," *IEEE Trans. Microwave Theory Tech.*, vol. MTT-16, pp. 529–535, Aug. 1968.

[4] E. Yamashita and K. Atsuki, "Distributed capacitance of a thin-film electrooptic light modulator," *IEEE Trans. Microwave Theory Tech.*, vol. MTT-23, pp. 177–178, Jan. 1975.

[5] T. G. Bryant and J. A. Weiss, "Parameters of microstrip transmission lines and of coupled pairs of microstrip lines," *IEEE Trans. Microwave Theory Tech.*, vol. MTT-16, pp. 1021–1027, Dec. 1968.

[6] S. V. Judd, I. Whiteley, R. J. Clowes, and D. C. Rickard, "An analytical method for calculating microstrip transmission line parameters," *IEEE Trans. Microwave Theory Tech.*, vol. MTT-18, pp. 78–87, Feb. 1970.

[7] W. T. Weeks, "Calculation of coefficients of capacitance of multiconductor transmission lines in the presence of a dielectric interface," *IEEE Trans. Microwave Theory Tech.*, vol. MTT-19, pp. 35–43, Jan. 1970.

[8] R. Mittra and T. Itoh, "A new technique for the analysis of the dispersion characteristics of microstrip lines," *IEEE Trans. Microwave Theory Tech.*, vol. MTT-19, pp. 47–56, Jan. 1971.

[9] P. Daly, "Hybrid-mode analysis of microstrip by finite-element methods," *IEEE Trans. Microwave Theory Tech.*, vol. MTT-19, pp. 19–25, Jan. 1971.

[10] D. G. Corr and J. B. Davies, "Computer analysis of the fundamental and higher order modes in single and coupled microstrip," *IEEE Trans. Microwave Theory Tech.*, vol. MTT-20, pp. 669–678, Oct. 1972.

[11] M. K. Krage and G. I. Haddad, "Frequency-dependent characteristics of microstrip transmission lines," *IEEE Trans. Microwave Theory Tech.*, vol. MTT-20, pp. 678–688, Oct. 1972.

[12] E. J. Denlinger, "A frequency dependent solution for microstrip transmission lines," *IEEE Trans. Microwave Theory Tech.*, vol. MTT-19, pp. 30–39, Jan. 1971.

[13] M. K. Krage and G. I. Haddad, "Characteristics of coupled microstrip transmission lines—II: Evaluation of coupled-line parameters," *IEEE Trans. Microwave Theory Tech.*, vol. MTT-18, pp. 222–228, Apr. 1970.

[14] R. P. Owens, J. E. Aitken, and T. C. Edwards, "Quasi-static characteristics of microstrip on an anisotropic sapphire substrate," *IEEE Trans. Microwave Theory Tech.*, vol. MTT-24, pp. 499–505, Aug. 1976.

[15] T. Edwards and R. P. Owens, "2–18 GHz dispersion measurements on 10–100 Ω microstrip lines on sapphire," *IEEE Trans. Microwave Theory Tech.*, vol. MTT-24, pp. 506–513, Aug. 1976.

[16] J. A. Weiss and T. G. Bryant, "Dielectric Green's function for parameters of microstrip," *Electron. Lett.*, vol. 6, no. 15, pp. 462–463, July 1970.

[17] N. G. Alexopoulos, C. Krowne, and S. Kerner, "Dispersionless coupled microstrip over fused silica-like anisotropic substrates," *Electron. Lett.*, vol. 12, no. 22, pp. 579–580, Oct. 28, 1976.

[18] T. C. Bryant and J. A. Weiss, "MSTRIP (parameters of microstrip); Computer program description," *IEEE Trans. Microwave Theory Tech.*, vol. MTT-19, pp. 418–419, 1971.

[19] E. G. Cristal, "Coupled-transmission-line directional couplers with coupled lines of unequal characteristic impedances," *IEEE Trans. Microwave Theory Tech.*, vol. MTT-14, pp. 337–346, July 1966.

[20] C. M. Krowne, "Microstrip transmission lines on pyrolytic boron nitride," *Electron. Lett.*, vol. 12, no. 24, pp. 642–643, Nov. 25, 1976.